ESTIMATION OF THERMAL PERFORMANCE OF PV-ETFE CUSHION ROOF

J. H. HU *, W. J. CHEN*, B. Zhao*, Q.Y. CAI*, Z.Y. QIU* and H. SONG†

* Space Structures Research Center, Shanghai Jiao Tong University, Shanghai 200240, China
E-mail: jtuhjh@gmail.com, cwj@sjtu.edu.cn, web page://www.ssrc.cn

† Shanghai Taiyokogyo Co., Ltd, Shanghai 200030, China
E-mail: songhao@taiyokogyo.com.cn, Web page: http://www. taiyokogyo.com.cn

Key words: Amorphous Silicon Photovoltaic; Computational Fluid Dynamics; PV-ETFE Cushion Roof; Thermal Performance; Temperature Distribution; Velocity Distribution.

Summary. ETFE (ethylene tetrafluoroethylene) cushion roof integrated amorphous silicon photovoltaic (PV-ETFE cushion roof) is attractive as this roof could provide electricity for maintaining the shape of the ETFE cushion and make the building to be zero-energy. One of the essential factors for this cushion roof is the temperature which affects the system thermal performance. To investigate the temperature and velocity fields inside the PV-ETFE cushion, an experimental mock-up composed of a three-layer ETFE cushion and a-Si PV is developed and experiments for obtaining the temperatures of the cushion roof are carried out under summer sunny conditions. These experimental results could provide the boundary condition for the numerical simulation and for the numerical verification. In this paper, estimation of the temperature field inside the ETFE cushion is performed with the FLUENT and the numerical temperature is compared with the experimental air temperature obtained at the same location. The comparison shows that the maximum difference between the experimental and numerical temperature results is only 3.4 K, which means that the feasibility of the numerical simulation is validated. In detail, for the temperature distribution, it is found that the existence of the PV has a significant effect on the temperature field and that heat transfer mechanisms for the upper and lower chambers formed with the three ETFE layers are the convective and conduction, respectively. For the velocity distribution, the vertical velocity is much greater than the horizontal velocity due to the convective effect.

1 INTRODUCTION

Thermal performance in enclosed building facades or roofs is indispensable for understanding airflow patterns and obtaining high quality building performance from the viewpoint of heat transfer [1]. In this case, the requirement of the thermal performances to solve building physical problems has attracted considerable attention in recent decades due to the rapid development of the building structures [2] and the application of building integrated photovoltaic (BIPV) [3]. For these reasons, many researchers have focused on evaluating building thermal performances on different building types, such as the conventional and new buildings types.

For conventional buildings, main attention is paid to the facades and horizontal enclosures. Popa et al. estimated the velocity fields of a double-skin window in terms of the aspect ratio

and Rayleigh number on the structure of the flow and concluded that a recirculation zone was always observed at the exit of the channel [4]. von Grabe extended the study with a simulation algorithm to investigate the flow and temperature, and suggested that the flow conditions in a double facade were turbulent and the increase of air temperature was greater near the heat sources [5]. Murakami et al. presented a 3-D simulation of 3 different rooms and concluded that k-ε model could accurately predict the airflow in enclosed square rooms [6]. It could provide feasible methods and basic understanding for estimating thermal performance of new building types.

In recent decades, the building types have changed as the requirements of the energy saving and new building types have emerged with the development of materials and structure types [7, 8]. Typical structures are the membrane structure [9, 10], high performance concrete structure [11] and long-span steel structure [12]. Due to the material properties and building requirements, thermal performance of these structures is not well understood, especially for membrane structures. The membrane structure is commonly built with new membrane materials, for example ethylene tetrafluoroethylene (ETFE) [2]. The shape of ETFE structure is formed as the cushion with two or more ETFE layers welded at the perimeter and inflated by overpressure [9]. The light-transmittance of the ETFE is more than 90% and the cushion roof could have the potential to store heat due to the airtight capacity. Therefore, the ETFE cushion roofs are suitable for the green-house and stadium where adequate light and good thermal performance are necessary. As thermal performance is indispensable for evaluating building environment and performances, it is meaningful to investigate the performance for ETFE cushion roofs. For two-layer ETFE cushion roof, Poirazis et al. presented an energy model to estimate energy transmission and consumption for building applications [13]. Antretter et al. utilized a CFD method to access the temperature and velocity field in terms of temperature difference and inclinations [14]. These methods with reasonable modifications could be utilized to identify thermal performances of new types of ETFE cushions. In recent research, a three-layer ETFE cushion integrated amorphous silicon photovoltaic (a-Si PV) was proposed [3, 15-17]. It could solve the problem inherited in this structure that the maintenance of the cushion shape needs additional energy compared with other conventional buildings. Therefore, thermal performances of ETFE cushion roof integrated a-Si PV are significant but unavailable in the literature.

This paper investigates thermal performance of the three-layer ETFE cushion integrated a-Si PV with experiment and simulation. An experimental mock-up was built and corresponding temperatures on the cushion were obtained to provide the real boundary conditions for the numerical model and to validate the numerical results. The CFD method to simulate temperature and velocity fields inside the cushion was employed with specific changes to consider the a-Si PV and cushion roof. It is found that the experimental temperature was in good agreement with the corresponding location of numerical temperature. Therefore, the numerical results were justified and could be used to analyze the airflow characteristics. Finally, typical temperature characteristics and important values of thermal performances were summarized in the conclusions.

1. EXPERIMENTATION

1.1. Design considerations

For the integration, the a-Si PV horizontally integrated on the surface of the middle-layer of the three-layer ETFE cushion is based on the following considerations compared with two-layer ETFE cushions integrated a-Si PV [15]: Provide output electricity for system utilization and a way of collecting thermal energy; avoid the effects of weather conditions (wind and rain) on the PV and high PV temperature on structural ETFE layers (i.e. top and bottom layer). These characteristics of the PV-ETFE cushion roof mean that advantages of a-Si PV correspond well with the demands of ETFE cushion and the three-layer ETFE cushion is an appropriate way for the integration.

1.2. Experimental mock-up

An experimental mockup consists of an ETFE cushion roof, a solar energy control system (SECS) and a pressure control system (PCS), shown in Fig. 1. The working principle of the system is that the SECS provides electricity for the PCS to inflate the horizontally placed cushion to form and maintain its designed shape. The working principles of the subsystems are summarized as follows[15].

Table 1 Equipment specifications of the experimental mock-up.

Equipment	Type	Voltage/V	Current/A	Power/W
a-Si PV	PVL68	16.5	4.1	68[a]
Solar controller	EPIPC-COM	24	20	-[b]
Pressure sensor	KQ-SPB2088	24	20[c]	0.5
PLC	PM564-T	24	5	-
Blower	G1G160-BH29-52	24	5.8	105
Solenoid valve	ZQDF-1	24	-	20

[a] The unit of the power of a-Si PV is Wh.
[b] This symbol means that this parameter is not available from the Instructions.
[c] The unit of the current of pressure sensor is mA.

·   The ETFE cushion roof, composed of a three-layer ETFE cushion, aluminum clamps and EPDM (ethylene-propylene-diene monomer) rubber. The three-layer ETFE cushion with the dimensions of 2000 mm wide, 4000 mm long and 250 mm rise in the middle of the cushion is placed horizontally. On its middle layer, 100 mm holes are designed along the center line to make the same pressure of the two chambers formed by the three layers. Aluminum clamps and EPDM rubber are utilized to keep the airtight of the cushion.

·   The solar energy control system (SECS) is composed of a solar controller, two 394 mm×3000 mm a-Si PV panels. In this subsystem the solar controller plays the key role in energy management.

·   The pressure control system (PCS) include a pressure sensor, a programmable logic controller (PLC), a blower and solenoid valves. In this subsystem a pressure range of 240-360 Pa in the ETFE cushion is set and controlled by the PLC.

According to the system requirements, the equipment and device are listed in Table 1. The corresponding theoretical diagram and experimental mock-up are shown in Fig. 1.

An experiment was carried out on 15th August in 2012 under summer sunny condition. The reasons for selecting this weather condition are that the solar irradiance on rainy and cloudy

days is low and that the solar irradiance on sunny days is strong and typical for evaluating the maximum thermal performances of the ETFE cushion roof integrated a-Si PV.
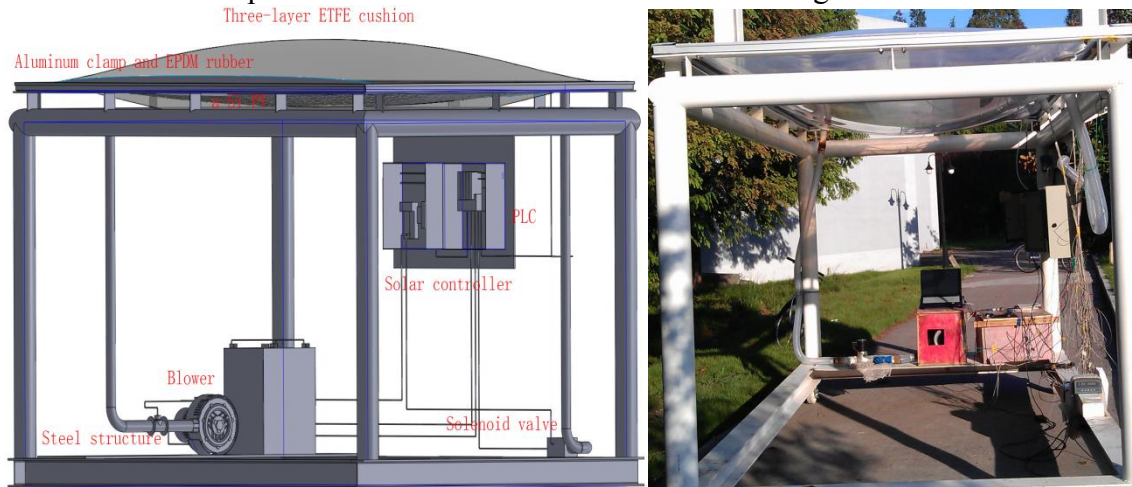

Fig. 1 Schematic diagram and experimental photo of the experimental mock-up

1.3. Experimental results

The measured data are the solar irradiance and the temperatures of the a-Si PV, top layer, middle layer, bottom layer and air inside the cushion. All data are shown in Fig. 2 with the time interval of an hour. The selection of the time period of 11:30-12:30 under summer sunny condition is because the weather condition was approximately stable, which is the requirement of the assumed steady state presented in the simulation. This is justified by the solar irradiance curve as its maximum fluctuation was only 30 W/m^2 and the ratio of this fluctuation to the solar irradiance was less than 1/30.

From Fig. 2, the a-Si PV temperature due to the photothermal effect was much greater than other temperatures. It is the main difference between cushions integrated a-Si PV and conventional cushions and needs to be considered to evaluate the thermal performances of the ETFE cushion roof. The temperature sequence of the three layers was the middle layer, top layer and bottom layer within this time period. The reasons are as follows:

·   The middle layer was affected by two main factors, i.e. solar irradiance and air temperature inside the cushion. In detail, the solar irradiance can be almost the same as outside since the transmittance of the ETFE is more than 90% (see Table 2). Meanwhile, the heated air could reduce the convection of the middle layer. Therefore, the temperature of the middle layer was the highest.

·   For the top layer, the solar irradiance on the external surface was almost the same as the middle layer and the air inside the cushion can prevent the convection to the internal surface. However, wind on external surface could accelerate external surface convection. Therefore, the temperature of the top layer was lower than that of the middle layer.

·   For the bottom layer, the solar irradiance reaching the surface was reduced by the two layers and absorbed by the a-Si PV. Moreover, the wind on the external surface could also accelerate the convection. As a result, the temperature was the lowest.

The air temperature inside the cushion was found to be within the range of the top and middle layers. This is plausible as the measured location was between these two layers. In fact,

the air temperature inside the cushion is the main focus of this experimental verification since this temperature is used for comparison with numerical results.

As this subsection focuses on the temperature characteristics, the temperature value and the comparisons with the numerical results are summarized and presented in the following sections.
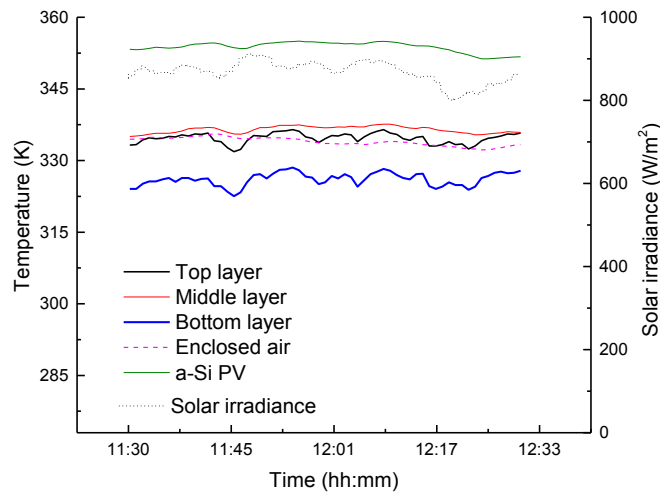

Fig. 2 Measures temperatures varying with the solar irradiance

2. NUMERICAL MODELING

2.1. Physical model setup

A simplified but appropriate model could produce reasonable numerical results compared with experimental results. The simplicity needs to eliminate the complexity and unnecessary parts but include typical building characteristics. Meanwhile, the appropriate treatment of the numerical model could reproduce main profiles and values obtained from experimental results. Therefore, special attention needs to be paid to the ETFE material and cushion type as the thermal properties of ETFE are not available in numerical software and temperature boundary conditions of the three-layer ETFE cushion are complex.

In this study, the thermal performance of the cushion is the main purpose and a two dimensional (2-D) model (see Fig. 3) was established as investigation on thermal performances of the ETFE cushion integrated a-Si PV is unavailable. The width and the rise of the cushion were set to be 2000 mm and 250 mm which were the real geometries of the cushion roof. Two PVs with the width of 394 mm were symmetrically distributed on the surface of the middle layer. A distance of 100 mm was applied in the center of the middle layer to simulate the holes which were utilized to guarantee the equal pressure between the upper and lower chambers. In this paper, the numerical simulation was performed under summer sunny condition which represented the maximum condition for evaluating the thermal performances of the cushion roof.

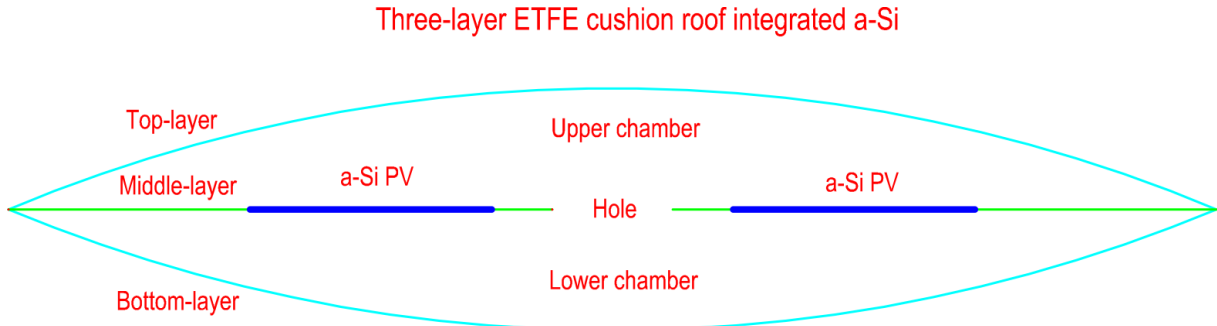**Three-layer ETFE cushion roof integrated a-Si**

Fig. 3 Two dimensional (2-D) numerical model of the three-layer ETFE cushion roof integrated a-Si PV

2.2. Governing equations

As stated previously, the physical model in this study is 2-D of the three-layer ETFE cushion integrated a-Si PV. To estimate the thermal performances effectively, the governing equations need to consider the following assumptions and approximations.

The PV is simplified to be the temperature and heat flux as this study intends to obtain the thermal profiles of the ETFE cushion; Steady state flow inside the cushion; this is verified under sunny days with approximately stable solar irradiance; Turbulence flow pattern; it is plausible under the consideration of the high temperature and curved surface [14]; Boundary conditions are directly applied to the surface to simplify the interactions between the cushion roof and surroundings; The radiation model is chosen to be the P1 model because the P1 model belongs to the spherical harmonics method used to solve the radiative transfer equation (RTE) [18]; All properties are assumed to be constant except that the effect of density variation on buoyancy is retained with the Boussinesq approximation [19].

Therefore, the 2-D steady state, incompressible turbulent flow model is employed in this study and the governing equations are as follows [20].

Continuity

$$\frac{\partial u}{\partial x} + \frac{\partial v}{\partial y} = 0 \tag{1}$$

X-momentum

$$\rho u \frac{\partial u}{\partial x} + \rho v \frac{\partial u}{\partial y} = -\frac{\partial p}{\partial x} + \mu \nabla^2 u \tag{2}$$

Y-momentum

$$\rho u \frac{\partial v}{\partial x} + \rho v \frac{\partial v}{\partial y} = -\frac{\partial p}{\partial y} + \mu \nabla^2 v + \rho \beta g (t - t_c) \tag{3}$$

Energy

$$\rho u \frac{\partial t}{\partial x} + \rho v \frac{\partial t}{\partial y} = \frac{k}{c_p} \nabla^2 t \tag{4}$$

where u and v are the velocities in x and y directions. p and ρ are the pressure and air density. t and t_c are the temperatures of air and bottom layer. μ, β, g, k and c_p are the

dynamic viscosity, volumetric expansion coefficient, gravity acceleration, thermal conductivity and specific heat (see Table 3).

2.3. Boundary conditions

The boundary conditions play an important role for the field distribution in enclosed spaces. Appropriate simplification could facilitate simulations and obtain reasonable results. In this study, the boundary conditions are simplified with the following considerations.

· Surface shape. Abanto et al. showed that the surface shape affected the field distribution significantly [21]. This means that the utilization of the two plates to replace the two-layer ETFE cushion is not sufficient to get the accurate results [22]. Therefore, the curved surface is employed and the boundary conditions are directly applied on the surface because the simulation is used to obtain the field distribution.

· PV temperature is simplified as the temperature with the heat flux. The temperature is the experimental results and the heat flux is obtained from [23]. Moreover, temperatures on the middle layer and the air inside the cushion are also based on experimental results.

· Thermal properties; these parameters in Table 2 are validated by available simulations [14, 22] or supplied by the supplier [24].

Table 2 Main physical and thermal properties of ETFE

Parameter	Unit	Value
Light transmission	%	90-97
Use temperature	^{o}C	-200 to 150
Thermal conductivity	W/(m·K)	0.16
Heat capacity	J/(kg·K)	2303

Table 3 Parameter values for the governing equations

Parameter	Unit	Value
β	$1/K$	3.0×10^{-3}
v	m^2/s	1.7×10^{-5}
α	m^2/s	1.9×10^{-5}
k	$W/(m \cdot K)$	2.7×10^{-2}
c_p	$kJ/(kg \cdot K)$	1.005
g	m/s^2	9.81

2.4. Numerical methods

Eqs. (1)-(4) are discretized using staggered, non-uniform control volume. The velocity components are defined at the center of the mesh edge and scalar qualities are set in the center of the mesh. For the momentum equations, the centered difference scheme is adopted for the convective term. The QUICK (quadratic upstream interpolation for convective kinematics) is used to remove the oscillation caused by the numerical instability [25]. As the velocities are coupled with the pressure, the SIMPLE (semi-implicit method pressure linked equation) algorithm is suggested by Patankar [26]. The discretization of the pressure correction equations results in a set of equations with symmetrical coefficient matrix which is solved by

the conjugate gradient method [27]. To ensure the convergence of the numerical algorithm, the following criterion is applied to all dependent variables over the solution domain [19].

$$\sum \left| \phi_{i,j}^{m} - \phi_{i,j}^{m-1} \right| \leq 10^{-3} \tag{5}$$

where ϕ represents a dependent variable of *U, V, P* and *T*. The indexes *i, j* indicate a grid point and the index *m* donates the current iteration at the finest grid level.

On the basis of these settings, the simulations are performed with the software FLUENT and conducted until the converged solutions are obtained.

2.5. Numerical results

The estimation of the thermal performances in horizontal space mainly needs the temperature and velocity fields. These parameters could reveal a basic understanding of the heat transfer mechanisms, including convective, conduction and radiation as well as the interactions between them. The numerical results could help to understand the dependency of the transport mechanisms. For these reasons, this subsection analyzes the above mentioned parameters in the three-layer ETFE cushion roof integrated a-Si PV.

2.5.1. Temperature field

Temperature difference resulting from that the gravity counteracts the buoyancy forces are the driving forces for the natural convection. Therefore, the main focus in this subsection is to understand the airflow pattern with reasonable explanations.

The temperature distribution in the three-layer ETFE cushion is shown in Fig. 4, which is expressed in filled isotherm pattern. The main characteristic is that a significant temperature gradient existed and decreased dramatically with the distance from the PV. This means that the existence of the PV greatly changed the temperature field inside the cushions to be complex. To understand the complexity based on the conclusion that the temperature difference has a significant effect on the temperature distribution [28], the temperature analysis needs to consider the temperature differences in the upper and lower chambers.
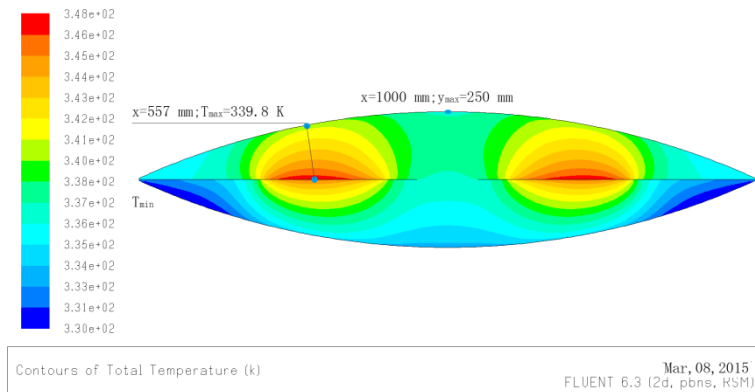

Fig. 4 Temperature distribution inside the three-layer ETFE cushion roof

It is found that the temperature difference between the PV and the top layer was positive, which is the reason to generate the natural convection. As shown in Fig. 4, the maximum temperature was 339.8 K at x=557 mm where the distance between the center of the a-Si PV and the top layer is the minimum. However, this location is not the summit of the ETFE

cushion (x=1000 mm; T=336.9 K), which means that structural analysis needs to consider the maximum temperature for appropriately understanding structural performances.

The temperature in the lower chamber was not as significant as that in the upper chamber since the difference between the bottom layer and the PV was negative. In this case, the main transport mechanism could be conduction which was not as strong as the convective effect [14]. As the main transport mechanism was the conduction, another interesting observation is that the lowest temperature was near the corner of the lower chamber. The reasons are that the effect of the PV on the temperature decreased with the distance and the air in the lower chamber was less mixed because of the conduction. These two effects might get balanced at the corner of the cushion, resulting in the minimum temperature.

The above temperature characteristics are useful to understand the transport mechanisms inside the cushion.

2.5.2. Velocity filed

The velocity is composed of components in x and y directions. The x velocity is resulting from the circulating of the air in the cushion caused by the natural convection. In detail, the air near the PV obtains energy and rises as the temperature gets high. This rising temperature drives the upper air to move and the area from the rising air is filled with the surrounding low temperature. These effects form the air circulation where the energy transmission exists.

The y velocity is shown in Fig. 5. It is found that the velocity distribution was a little more uniform in the upper chamber than that in the lower chamber, resulting in smaller temperature gradient. For the velocity magnitude, the maximum velocity was around the PV and the minimum was in the lower chamber. The x velocity was the secondary velocity as the maximum velocities in y and x direction were 2.60×10^{-3} and 1.35×10^{-3} m/s, respectively.

The velocity profile explains the temperature distribution from another perspective. Moreover, it gives the basic understanding of the air inside the cushion and is useful for further 3-D simulation.
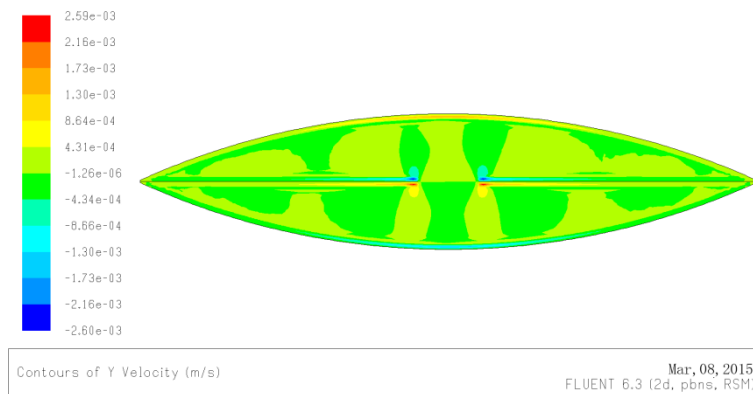

Fig. 5 Velocity distribution in y-direction inside the three-layer ETFE cushion roof

2.6. Discussions

The experimental results show that the air temperature inside the ETFE cushion was stable within the selected time period and the average temperature was 334 K. On the other side, the numerical result of the temperature at the same location was 337.4 K. The ratio of the

temperature difference to the measured temperature was only 5.5%, which justifies that the numerical models with the mentioned assumptions are reasonable.

3. CONCLUSIONS

This paper concerns thermal performances of the three-layer ETFE cushion roof integrated a-Si PV, such as the temperature distribution and velocity distribution. To investigate these thermal performances, field experiments and numerical modeling with real boundary conditions were performed and compared in this paper.

The experimental results show that the temperature sequence of the three layers was the middle, top and bottom layer and that the PV temperature was 353.8 K. This gives evidence that the PV has a significant effect on the temperature distribution. The experimental temperature was in good agreement with the corresponding location of numerical temperature since the maximum temperature difference was only 3.4 K. Therefore, the numerical results were justified and then used to analyze the flow characteristics. In detail, it is found that the main transport mechanisms in the upper and lower chambers formed by the three layers were the convection and conduction, respectively. The maximum temperature near the surface of the cushion was 339.8 K at the location of x=557 mm where the distance between the center of the a-Si PV and the top layer was the minimum. Moreover, the vertical velocity was greater than horizontal velocity due to the convective effect.

References

[1] Khalifa A-JN. Natural convective heat transfer coefficient–a review: II. Surfaces in two- and three-dimensional enclosures. Energy Conversion and Management. 2001;42(4):505-17.

[2] Robinson-Gayle S, Kolokotroni M, Cripps A, Tanno S. ETFE foil cushions in roofs and atria. Construction and Building Materials. 2001;15(7):323-7.

[3] Chen W, Hu J, Song H. Novel BIPV/T ETFE cushion. Textile Composites and Inflatable Structures 2013. p. 363-74.

[4] Popa C, Ospir D, Fohanno S, Chereches C. Numerical simulation of dynamical aspects of natural convection flow in a double-skin façade. Energy and Buildings. 2012.

[5] von Grabe J. A prediction tool for the temperature field of double facades. Energy and Buildings. 2002;34(9):891-9.

[6] Murakami S, Kato S. Numerical and experimental study on room airflow—3-D predictions using the k-ϵ turbulence model. Building and Environment. 1989;24(1):85-97.

[7] Ziapour BM, Palideh V, Baygan M. Performance comparison of four passive types of photovoltaic–thermal systems. Energy Conversion and Management. 2014;88:732-8.

[8] Adaramola MS, Vågnes EE. Preliminary assessment of a small-scale rooftop PV-grid tied in Norwegian climatic conditions. Energy Conversion and Management. 2015;90:458-65.

[9] Chen W. Design of membrane structure engineering: China building industry press; 2005.

[10] Moritz K. ETFE-Folie als Tragelement. Germany: Technische Universität München; 2007.

[11] Aıtcin P. The durability characteristics of high performance concrete: a review. Cement and Concrete Composites. 2003;25(4):409-20.

[12] Zhao X-L, Zhang L. State-of-the-art review on FRP strengthened steel structures. Engineering Structures. 2007;29(8):1808-23.

[13] Poirazis H, Kragh M, Hogg C. Energy modelling of ETFE membranes in building applications. Eleventh International IBPSA Conference. Glasgow, Scotland2009.

[14] Antretter F, FH MED-I, Haupt W, Holm A. Thermal transfer through membrane cushions analyzed by computational fluid dynamics. 8th Nordic Symposium on Building Physics in the Nordic Countries Copenhagen, Lyngby2008. p. 347-54.

[15] Hu J, Chen W, Zhao B, Song H. Experimental studies on summer performance and feasibility of a BIPV/T ethylene tetrafluoroethylene (ETFE) cushion structure system. Energy and Buildings. 2014;69:394-406.

[16] Hu J, Chen W, Zhao B, Song H. Experimental studies on system performance of PV-ETFE cushionsystem in winter. Journal of Zhejiang University 2014;48(10):1816-21.

[17] Hu J, Chen W, Zhao B, Hu P, Ge B, Song H. Numerical and experimental study on a thermal model of flexible amorphous silicon thin film photovoltaic panels. Journal of Shanghai Jiao Tong University. 2015;49(4):19-24.

[18] Lee I, Short T. Two-dimensional numerical simulation of natural ventilation in a multi-span greenhouse. Transactions of the ASAE. 2000;43(3):745-53.

[19] Sezai I, Mohamad A. Natural convection from a discrete heat source on the bottom of a horizontal enclosure. International Journal of Heat and Mass Transfer. 2000;43(13):2257-66.

[20] Incropera FP. Fundamentals of heat and mass transfer: John Wiley; 2007.

[21] Abanto J, Barrero D, Reggio M, Ozell Bt. Airflow modelling in a computer room. Building and Environment. 2004;39(12):1393-402.

[22] Dimitriadou EA, Shea A. Computational modelling of the thermal behaviour of an ETFE cushion using IES. Sustainable Building 2013. p. 175-81.

[23] Chen F, Wittkopf SK, Khai Ng P, Du H. Solar heat gain coefficient measurement of semi-transparent photovoltaic modules with indoor calorimetric hot box and solar simulator. Energy and Buildings. 2012;53:74-84.

[24] Uni-solar Technical Report. United Solar Ovonic; 2006.

[25] Leonard BP. A stable and accurate convective modelling procedure based on quadratic upstream interpolation. Computer methods in applied mechanics and engineering. 1979;19(1):59-98.

[26] Patankar SV. Numerical Heat Transfer and Fluid Flow. New York: McGraw-Hill; 1980.

[27] Hackbush W. Iterative Solution of Large Sparse System of Equations. New York: Springer-Verlag; 1994.

[28] Antretter F. Anwendung eines Computational-Fluid-Dynamic-Systems zur numerischen Simulation der natürlichen Konvektion in leichten transparenten Bauteilen: Fraunhofer-Institut für Bauphysik; 2007.